JOC The Journal of Organic Chemistry

Article

pubs.acs.org/joc

Reaction Pathway and Free Energy Profile for Conversion of π-Conjugation Modes in Porphyrin Isomer

Takashi Matsuo,*[,†] Yuji Tohi,[‡] and Takashi Hayashi*[,‡]

[†]Graduate School of Materials Science, Nara Institute of Science and Technology (NAIST), Ikoma, Nara 630-0192, Japan

[‡]Department of Applied Chemistry, Graduate School of Engineering, Osaka University, Suita, Osaka 565-0871, Japan

Supporting Information

ABSTRACT: Porphycene is a structural isomer of porphyrin with 18π-conjugated aromatic character. Porphycene modified with trifluoromethyl (CF_3) groups in the periphery of the framework readily affords the isolable 20π-conjugated antiaromatic form through a reaction with a proton-donating reductant. The 20π-conjugated form can be characterized by not only a variety of spectroscopies in solutions but also X-ray crystallography. This paper focuses on the free energy profile in the conversion of the 18π-conjugated porphycene into the 20π-conjugated form. From the results of kinetics, electrochemical measurements, and acid/base titrations, the 20π-conjugated CF_3 porphycene is formed by a concerted proton−electron transfer (CPET) from a hydroquinone reagent to the 18π-conjugated form. The hydrogen-atom affinity of the 18π-conjugated CF_3 porphycene (for two hydrogen atoms) was calculated to be −490 kJ mol^{-1}, indicating that the N−H bonds in the 20π-conjugated form are rather easily cleaved. This reflects the antiaromatic characteristics of the 20π-conjugated porphycene. We propose that the kinetic and thermochemical analysis using redox potentials and pK_a data is applicable for determining the reaction pathway in conversion of aromatic/antiaromatic mode of π-conjugated macrocycles as well as popular investigations for oxidations of organic molecules.

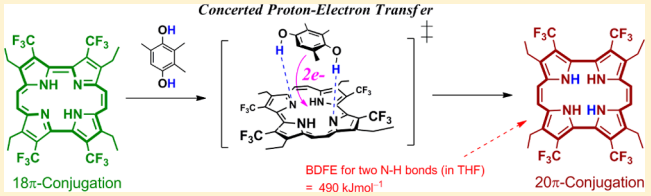

INTRODUCTION

Since chemical and optical properties of aromatic macrocycles are reflected by their π-circular conjugation modes, modulation of the π-conjugation modes is of importance to develop macrocycles with desired physicochemical properties.[1,2] One of the typical approaches is the introduction of substituent groups in the periphery of the parent macrocycle. When a macrocycle is composed of several small aromatic subunits (e.g., porphyrin), reconstitution of arrangement of subunits is also useful. This method involves ring expansion/contraction and ring isomerization.[2−8] However, most of the π-conjugated macrocycles constructed by these methods still retain aromaticity, a basic character provided by the $(4n + 2)$ π-circular conjugation system. In this regard, perturbation of aromaticity will give us another unique strategy to dramatically alter the characteristics of π-conjugated macrocycles, which is quite different from the typical and popular approaches described above. The subject is related with construction of nonaromatic/antiaromatic π-conjugated macrocycles. In the chemistry of porphyrinoids (porphyrins and porphyrin-related compounds), macrocyles with these π-conjugation modes have been extensively studied from thoretical and experimental aspects.[8−15] Nonclassical aromatic porphyrinoids (e.g., topological porphyrinoids with Möbius aromaticity) have also been reported.[16,17]

In order to quantitatively evaluate the stability and the availability of macrocycles with unusual π-conjugation modes, a useful approach is study of thermochemical profiles between two macrocycles with similar ring sizes, in which aromaticity is attained in one compound and lost in another. Employment of similar-sized compounds is indispensable because the difference in stabilities between aromatic and nonaromatic macrocycles depends of their ring sizes.[3] In order to develop a procedure for evaluating free energy profiles in macrocycles from the viewpoint of π-conjugation modes, we focused on a set of 18π/20π-conjugated porphyrinoids where both compounds are composed of four pyrrole units.

20π-conjugated porphyrinoids belong to a family of compounds most structurally similar to the 18π-conjugated porphyrins. It has been believed that isolation of the 20π-conjugated porphyrins is rather difficult, as demonstrated by the isopholorin preparation reported by Woodward.[18] This is because such compounds are easily oxidized in air and are converted into the parent 18π-conjugated porphyrins. However, some research groups have successfully overcome this problem and isolated 20π-conjugated porphyrinoids after controlling the LUMO energy level in the ring[13] or by modifying the shape of the macrocycle.[19]

We have previously reported that the reaction of trifluoromethylated (CF_3) porphycene $\mathbf{1}_{\text{-H}_2}$ with a proton-donating reduction system (e.g., hydroquinone, Bu_3SnH + CF_3COOH, or $Na_2S_2O_4$+H_2O, etc.) yields an isolable 20π-conjugated porphycene $\mathbf{2}_{\text{-H}_4}$ (see Chart 1 where "**1**" and "**2**"

Received: July 2, 2012
Published: October 1, 2012

dx.doi.org/10.1021/jo3013379 | J. Org. Chem. 2012, 77, 8946−8955

Chart 1. Structures of 18π-Conjugated Trifluoromethylated Porphycene 1_{-H_2} and 20π-Conjugated Form 2_{-H_4}[a]

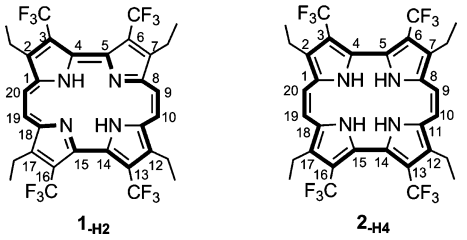

[a]Bold lines indicate the π-conjugation fashion. In 1_{-H_2}, only one of the two tautomers with respect to π-conjugation fashion is shown.

represent 18π- and 20π-conjugated CF_3 porphycene, respectively. A subscript with the compound name, "-H_X", denotes the number of hydrogen atoms bound to the inner nitrogen atoms).[20] A recent theoretical research disclosed that 2_{-H_4} has weak antiaromatic character.[21]

The 20π-conjugated CF_3 porphycene is produced by injection of two protons and two electrons into the parental 18π-conjugated porphycene. This provides us with a good opportunity to discuss the reaction pathway from the 18π-conjugated porphycene to the 20π-conjugated form, including a stepwise electron-and-proton transfer, or a concerted proton–electron transfer (CPET). This kind of investigation has often been carried out to characterize C–H, O–H, and N–H oxidations,[22,23] where thermochemical calculations using redox potentials and pK_a values of reactants, intermediates and products are employed to determine the most favorable reaction pathway. The free energy change can also be evaluated throughout the discussion. The investigation would be useful for predicting the experimental availability of designed compounds. In this paper, we apply this strategy for determination of the reaction pathway from 1_{-H_2} to produce 2_{-H_4} with accompanying conversion in the 18/20π-conjugation mode. Throughout the work, substituted hydroquinones were employed because they are formal $2H^+$-and-$2e^-$ donors. Furthermore, the profile of the free energy change in the conversion of the π-conjugation fashion will also be demonstrated, based on the procedure proposed by Bordwell[24,25] and Parker.[26,27]

RESULTS

Characterization of 2_{-H_4} in THF. On the addition of 2,3,5-trimethylhydroquinone (TMHQ) or monomethylhydroquinone (MMHQ) to 1_{-H_2} in THF, the absorption bands of 1_{-H_2} at 375 nm and in the region of 600–800 nm distinctly decreased and the new bands appeared at 323 nm (the spectral change for the reaction with TMHQ is shown in Figure 1(a) as a representative example). On the basis of the previous observation of similar spectral change in CH_2Cl_2,[20] the formation of 2_{-H_4} in THF was confirmed (Scheme 1).

The UV–vis titration experiment indicates the stoichiometry of 1:1 (Figure 1b). The stoichiometry was also investigated by ^{1}H NMR spectroscopy (Figure S1, Supporting Information). Compound 2_{-H_4} is sufficiently stable under the air, and the purification by a conventional column chromatography is possible.[20] In the ^{1}H NMR spectrum of 2_{-H_4} in THF-d_8, the pyrrolic NH protons appear at 11.36 ppm, whereas the

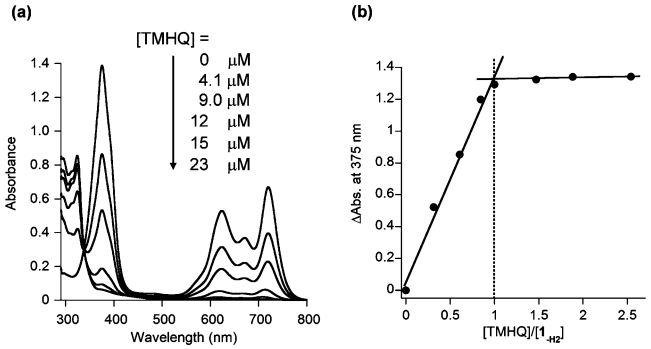

Figure 1. UV–vis spectral changes during the reaction of 1_{-H_2} (15 μM) with 2,3,5-trimethylhydroquinone (TMHQ) in THF under a N_2 atmosphere at 25 °C: (a) spectra obtained at 22 h after addition of various concentrations of TMHQ (dilution effect was calibrated); (b) plot of decrease in the absorbance at 375 nm vs [TMHQ]/[1_{-H_2}].

Scheme 1. Conversion of 18π-Porphycene 1_{-H_2} into 20π-Porphycene 2_{-H_4} by Substituted Hydroquinones

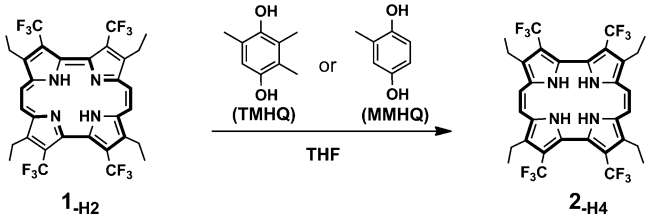

corresponding peaks are observed around 2.3 ppm for 1_{-H_2}.[28,29] These spectroscopic differences between 1_{-H_2} and 2_{-H_4} indicate the significant perturbation in the π-conjugation mode of the porphycene ring. The chemical shift of the pyrrolic NH protons of 2_{-H_4} in THF is lower than that previously reported in CD_2Cl_2 (9.45 ppm). This is because the pyrrolic protons form hydrogen bonds with solvent molecules. The [(pyrrole)N–H---O(THF)] hydrogen bonding was also observed in the previous X-ray crystallographic analysis for of 2_{-H_4}.[20]

Kinetics for Reaction of Porphycene 1_{-H_2} with Hydroquinone Reagent. A typical UV–vis spectral change which occurs during the reaction of porphycene 1_{-H_2} with excess TMHQ in THF is shown in Figure 2a. The absorbance change at 720 nm (Figure 2a inset) was analyzed by a single-phase kinetics law. The pseudo-first-order rate constants are linearly dependent on concentration of TMHQ (Figure 2b). Similar spectral changes were also observed in the reaction of 1_{-H_2} with MMHQ (Figure S2, Supporting Information). The first-order rate constants and the primary kinetic isotope effect (KIE) determined are summarized in Table 1 (see Figure S3, Supporting Information, for the absorbance changes in the KIE experiments). The first-order rate constant for the reaction with TMHQ is larger than that for the reaction with MMHQ by 10-fold. This is caused by the higher reduction ability of TMHQ (vide infra). The observation of KIE in both of the reactions indicates that movement of hydrogen atoms is associated with a rate-determining step.

The activation parameters are also included in Table 1 (see the Eyring plot in Figure S4 of the Supporting Information). The larger rate constant in the reaction with TMHQ is dominated by the small activation enthalpy. The large absolute

dx.doi.org/10.1021/jo3013379 | J. Org. Chem. 2012, 77, 8946–8955

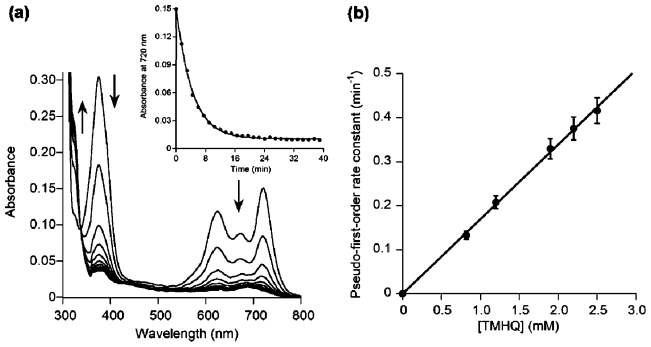

Figure 2. Kinetic analysis for the reaction of porphycene $\mathbf{1}_{\text{-H}_2}$ with trimethylhydroquinone (TMHQ) in THF under a N_2 atmosphere at 25 °C; (a) Transient spectra ($[\mathbf{1}_{\text{-H}_2}]$ = 3.5 μM, [TMHQ] = 1.2 mM, every 3 min over 40 min) and time-course of absorbance at 720 nm with a reaction curve obtained by single-phase kinetic analysis (inset); (b) Dependency of pseudofirst-order rate constants on [TMHQ].

Table 1. First-Order Rate Constants, Kinetic Isotope Effect (KIE), and Activation Parameters for Reactions of $\mathbf{1}_{\text{-H}_2}$ with Substituted Hydroquinones[a]

reaction	$\mathbf{1}_{\text{-H}_2}$ + TMHQ	$\mathbf{1}_{\text{-H}_2}$ + MMHQ
rate constant[b] (M^{-1} s^{-1})	2.8 ± 0.3	0.19 ± 0.02
KIE (= k_H/k_D)[c]	8.0 ± 0.9[d]	2.7 ± 0.3[e]
$\Delta H^{\ddagger}$ (kJ mol^{-1})	25 ± 2	47 ± 3
$\Delta S^{\ddagger}$ (J $mol^{-1}K^{-1}$)	−150 ± 21	−102 ± 19

[a]Under a N_2 atmosphere. [b]In THF at 25 °C. [c]In THF + 5% CH_3OH or 5% CD_3OD at 25 °C. The value of k_D was calculated on the basis of the deuterated ratio of a hydroquinone (see the Experimental section for details). [d]k_H = 0.49 min^{-1} and k_D = 0.061 min^{-1} at $[\mathbf{1}_{\text{-H}_2}]$ = 3.5 μM and [TMHQ] (or [deuterated TMHQ]) = 1.83 mM. [e]k_H = 0.19 min^{-1} and k_D = 0.071 min^{-1} at $[\mathbf{1}_{\text{-H}_2}]$ = 3.5 μM and [MMHQ] (or [deuterated MMHQ]) = 11.2 mM.

values in the activation entropies for both reactions suggest that the positioning of the reactants at the transition state is very significant for progress of the reaction.

Electrochemical Measurements. The activation enthalpies ($\Delta H^{\ddagger}$) for the formation of $\mathbf{2}_{\text{-H}_4}$ are reflected by the reduction ability of hydroquinone derivatives. The cyclic voltammograms for porphycene $\mathbf{1}_{\text{-H}_2}$ and the substituted hydroquinones obtained in THF are shown in Figure S5 (Supporting Information). The redox process of $\mathbf{1}_{\text{-H}_2}$ is shown in Scheme 2.

Porphycene $\mathbf{1}_{\text{-H}_2}$ exhibits a clear reversible voltammogram including the two redox waves. These redox waves are assigned as couples of $\mathbf{1}_{\text{-H}_2}/\mathbf{1}_{\text{-H}_2}^{\bullet-}$ (E_1 = +0.197 V vs SHE) and $\mathbf{1}_{\text{-H}_2}^{\bullet-}/\mathbf{1}_{\text{-H}_2}^{2-}$ (E_2 = −0.045 V vs SHE), respectively. The redox

Scheme 2. Redox Process of Porphycene $\mathbf{1}_{\text{-H}_2}$

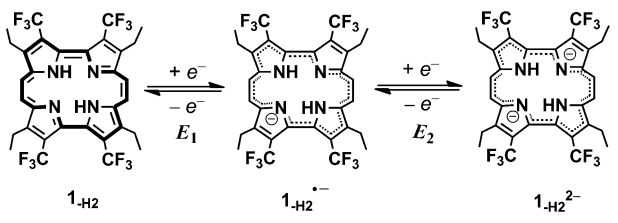

potentials are positively shifted from those for the previously reported etioporphycene and trifluoromethylated etio-type porphyrin.[20] This is resulted from the stabilization of the LUMO energy level in the low symmetric porphycene ligand and from the electron withdrawing effect by the CF_3 groups. In contrast, the voltammograms of the hydroquinones are not reversible (Figures S5(c) and S5(d), Supporting Information). When the electrode potential was scanned in the positive direction, an anodic wave was observed at +1.17 V vs SHE for TMHQ and +1.42 V for MMHQ. These waves are assignable as a one-electron oxidation coupled with deprotonation of the phenolic moieties (electron transfer-chemical reaction (EC) mechanism), which may be assigned as the oxidation to the benzoquinone form.[30] Proton dissociation-coupled oxidation generally occurs at more negative potentials than oxidation without deprotonation (formation of hydroquinone radical cation), since a radical cation is highly acidic.[31,32] Therefore, the limit of one-electron oxidation potential was defined as +1.17 V vs SHE for TMHQ and +1.42 V for MMHQ. The anodic shift in the oxidation potential of TMHQ is due to the increase in electron-donating effect by the methyl group in the benzene ring.

Acid Titration of Porphycene $\mathbf{1}_{\text{-H}_2}$. The KIE experiments suggested that the movement of hydrogen atoms from a hydroquinone to $\mathbf{1}_{\text{-H}_2}$ is associated with the rate-determining process. In order to evaluate the proton affinity of $\mathbf{1}_{\text{-H}_2}$, the protonation of the inner nitrogen atoms of $\mathbf{1}_{\text{-H}_2}$ (Scheme 3) by methanesulfonic acid (MSA) was observed by UV−vis spectral changes (Figure 3).

Scheme 3. Protonation onto 18π-Conjugated Porphycene $\mathbf{1}_{\text{-H}_2}$

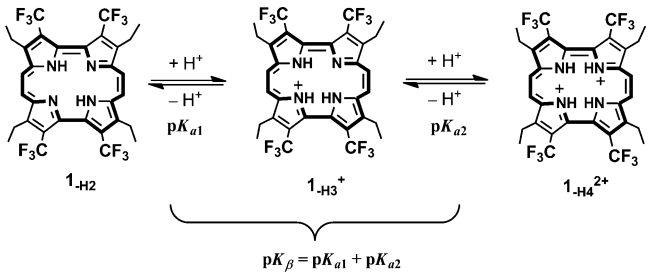

When the absorbance change was analyzed by a modified Hill equation (Figure 3b inset), the Hill coefficient was found

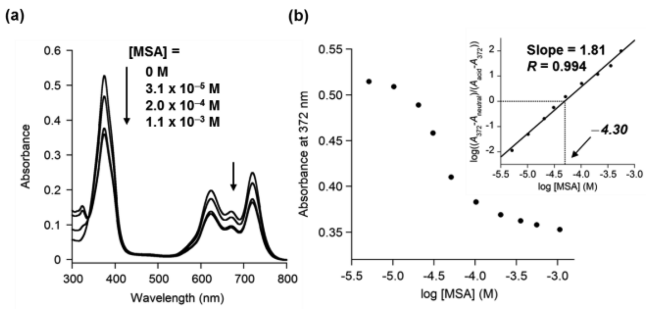

Figure 3. Acid titration of porphycene $\mathbf{1}_{\text{-H}_2}$ with methanesulfonic acid (MSA) in THF at 25 °C: (a) UV−vis spectral change during the titration; (b) absorbance change at 372 nm; (c) analysis by a modified Hill equation (eq 2) in the region of low MSA concentrations.

dx.doi.org/10.1021/jo3013379 | J. Org. Chem. 2012, 77, 8946−8955

to be $n \sim 2$, indicating that the experimentally available acid dissociation constant is the overall value involving the two protonation processes, K_β (= $K_{a1}K_{a2}$, see the derivation in the Experimental Section). With the reported pK_a(MSA) value in THF (= 13.53)[33] and the x-value at y = 0 of the Hill plot (= −4.3) pK_β = 22.13 is obtained.

Base Titration of Porphycene $\mathbf{2}_{\text{-H}_4}$ by DBU. The titration of 20π-conjugated porphycene $\mathbf{2}_{\text{-H}_4}$ with 1,8-diazabicyclo[5.4.0]-undec-7-ene (DBU) was also conducted (Scheme 4) The UV−vis changes in the reaction are shown in Figure 4.

Scheme 4. Deprotonation of 20π-Conjugated Porphycene $\mathbf{2}_{\text{-H}_4}$

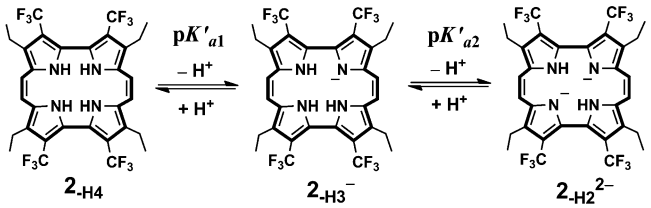

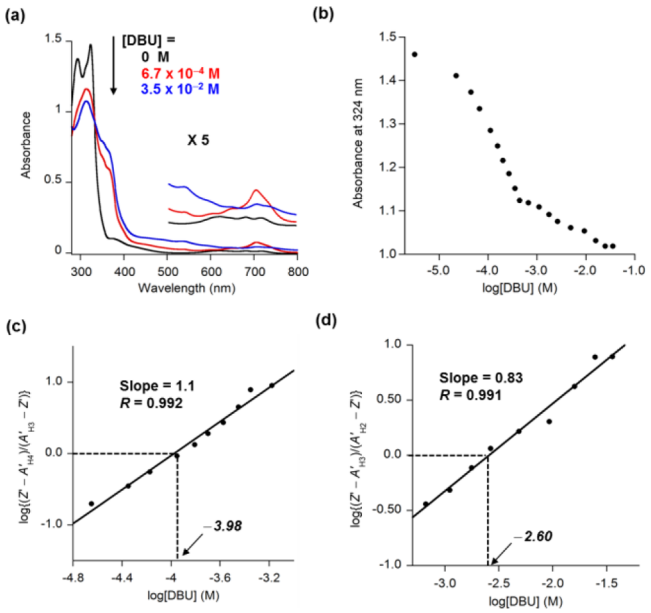

Figure 4. Base titration of porphycene $\mathbf{2}_{\text{-H}_4}$ with 1,8-diazabicyclo[5.4.0]undec-7-ene (DBU) in THF at 25 °C: (a) UV−vis spectral change during the titration (black line: [DBU] = 0, red line: [DBU] = 6.7 × 10^{-4} M, blue line: [DBU] = 3.5 × 10^{-2} M); (b) absorbance change at 324 nm; (c) analysis by a modified Hill equation (see the Experimental Section) in the region of low DBU concentrations; (d) analysis by a modified Hill equation in the region of high DBU concentrations.

The dependency of the absorbance at 324 nm on log[DBU] is composed of two phases. Each phase is assignable as a single-proton release with the first proton coming from $\mathbf{2}_{\text{-H}_4}$ (pK'_{a1}-process) and the second proton coming from $\mathbf{2}_{\text{-H3}}^{-}$ (pK'_{a2}-process). The analyses shown in parts c and d of Figure 4 afforded pK'_{a1} = 16.0 and pK'_{a2} = 17.4.

DFT Calculation of Free Energy Difference between Dianion Forms. Because the two-electron reduced form of $\mathbf{1}_{\text{-H}_2}$ and the doubly deprotonated form of $\mathbf{2}_{\text{-H}_4}$ (i.e., $\mathbf{1}_{\text{-H}_2}^{2-}$ and $\mathbf{2}_{\text{-H}_2}^{2-}$) are dianions with different π-circulation modes, it is possible for them to take their own favorable conformations. The DFT calculation for the total energies of the optimized geometries of $\mathbf{1}_{\text{-H}_2}^{2-}$ and $\mathbf{2}_{\text{-H}_4}^{2-}$ indicates that the difference in the optimized conformations between $\mathbf{1}_{\text{-H}_2}^{2-}$ and $\mathbf{2}_{\text{-H}_4}^{2-}$ is very small (see Figure S6, Supporting Information). The energetic difference between the two species is calculated to be 10.2 kJ mol^{-1}, which may be within the accuracy of DFT calculations.

DISCUSSION

Outlines of Reactions Yielding $\mathbf{2}_{\text{-H}_4}$. The UV−vis spectroscopic changes on the addition of a hydroquinone reagent to $\mathbf{1}_{\text{-H}_2}$ in THF (Figures 1 and 2 and Figure S1, Supporting Information) are very similar to those previously reported in the conversion of $\mathbf{1}_{\text{-H}_2}$ into $\mathbf{2}_{\text{-H}_4}$ by a proton-donating reduction in CH_2Cl_2.[20] This finding indicates that 20π-conjugated form, $\mathbf{2}_{\text{-H}_4}$, is available in THF under the same reaction conditions as those in CH_2Cl_2. According to the X-ray crystallographic investigation for $\mathbf{2}_{\text{-H}_4}$, the compound has a highly ruffled conformation, compared with $\mathbf{1}_{\text{-H}_2}$. Although the conformational character would weaken the efficiency of π-electron delocalization over the whole of the macrocycle, the previous theoretical investigation for $\mathbf{2}_{\text{-H}_4}$ proposed that the electronic delocalization is still attained and that $\mathbf{2}_{\text{-H}_4}$ has the character of an antiaromatic porphyrinoid rather than a nonaromatic compound.[21] This is supported by the NICS(0) parameter[34] of the compound (= +4.7), whereas the value for $\mathbf{1}_{\text{-H}_2}$ is −12.4.

The titration experiment confirms the 1:1 stoichiometry in the reaction of $\mathbf{1}_{\text{-H}_2}$ with TMHQ (Figure 1 and Figure S1, Supporting Information). This finding is consistent with the liner dependency of the pseudo-first-order rate constants on [TMHQ] (Figure 2). The absorbance difference mostly saturates on the addition of 1 equiv of TMHQ, and the conversion is evaluated to be ca. 93%.

Possible Pathways for Reaction of Porphycene $\mathbf{1}_{\text{-H}_2}$ with TMHQ. The formation of $\mathbf{2}_{\text{-H}_4}$ formally requires addition of two protons and two electrons to $\mathbf{1}_{\text{-H}_2}$. Scheme 5 depicts the possible modes of proton and electron transfers, where the vertical and horizontal directions indicate movements of protons and electrons, respectively.[22]

In the reaction of $\mathbf{1}_{\text{-H}_2}$ with a hydroquinone derivative, there are three possible reaction pathways: a sequential electron transfer-proton transfer (ET−PT), a sequential proton transfer-electron transfer (PT−ET), and a concerted proton−electron transfer (CPET).[35] These mechanisms correspond to paths A−C, respectively. As shown in Figure 2 and Figure S2, Supporting Information, accumulation of chemical intermediates was not observed. At first glance, it could be believed that the reaction proceeds with a one-step mechanism. However, it is impossible to simply address the reaction pathway because the two following possibilities are conceivable: (i) path A or B with a high activation energy barrier at the initial electron (or proton) transfer followed by the reaction with a relatively lower energy barrier or (ii) a one-step reaction as depicted in path C. The key parameter to determine the reaction pathway is the experimentally elucidated activation Gibbs energy: $\Delta G^{\ddagger} = \Delta H^{\ddagger} - T\Delta S^{\ddagger}$ = 70 kJ mol^{-1} for the reaction with TMHQ and 77 kJ mol^{-1} for the reaction with MMHQ (at 25 °C). Reaction

dx.doi.org/10.1021/jo3013379 | J. Org. Chem. 2012, 77, 8946−8955

Scheme 5. Possible Pathways for Conversion of $\mathbf{1}_{\text{-H}_2}$ into $\mathbf{2}_{\text{-H}_4}$

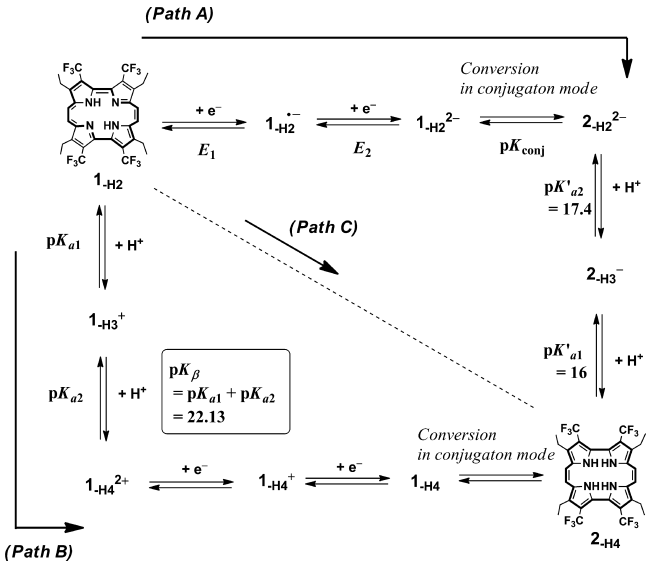

pathways with an activation barrier exceeding this value should be ruled out.

Reaction of Porphycene $\mathbf{1}_{\text{-H}_2}$ with Hydroquinone Proceeds with Concerted Mechanism. First, we investigate the possibility of path A (ET−PT mechanism). The first step in path A is one-electron reduction of $\mathbf{1_{H2}}$ by a hydroquinone (see Scheme 6). Calculated from the redox potential of $\mathbf{1}_{\text{-H}_2}/\mathbf{1}_{\text{-H}_2}^{\bullet-}$

Scheme 6. One-Electron Transfer from TMHQ to $\mathbf{1}_{\text{-H}_2}$

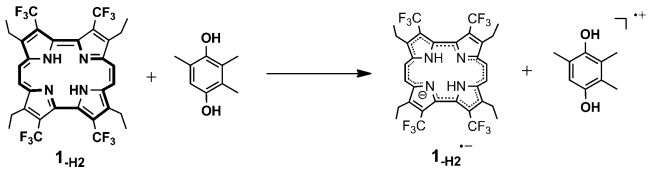

couple (E_1 = +0.197 V vs SHE) and the peak potential of TMHQ at an oxidation wave (= +1.17 V vs SHE), the electron transfer from TMHQ to $\mathbf{1_{H2}}$ is found to represent an uphill process by more than +0.973 V, corresponding to 93.9 kJ mol^{-1}. In the case of MMHQ, the energy barrier is calculated to be 118 kJ mol^{-1} at minimum. Since these values are much larger than the experimentally obtained activation barriers, the ET−PT mechanism is excluded.

Next, we consider the possibility of path B (PT−ET mechanism). The protonation process of $\mathbf{1}_{\text{-H}_2}$ by TMHQ is described in Scheme 7. The overall equilibrium constant ($K_{\text{1-H2-TMHQ}}$, equilibrium constant) and the overall acid dissociation constant of TMHQ ($K_{\text{TMHQ-all}}$) are as follows ((TMHQ-H)$^-$ and (TMHQ-2H)$^{2-}$ denote the single-deprotonated and double-deprotonated forms, respectively):

$$K_{\text{1-H2-TMHQ}} = [\mathbf{1}_{\text{-H}_4}{}^{2+}][(\text{TMHQ-2H})^{2-}]/[\mathbf{1}_{\text{-H}_2}][\text{TMHQ}] \quad (1)$$

$$K_{\text{TMHQ-1}} = [\text{H}^+][(\text{TMHQ-H})^-]/[\text{TMHQ}] \quad (2)$$

$$K_{\text{TMHQ-2}} = [\text{H}^+][(\text{TMHQ-2H})^{2-}]/[(\text{TMHQ-2H})^-] \quad (3)$$

$$K_{\text{TMHQ-all}} = K_{\text{TMHQ-1}}K_{\text{TMHQ-2}} = [\text{H}^+]^2[(\text{TMHQ-2H})^{2-}]/[\text{TMHQ}] \quad (4)$$

As $K_\beta = K_{a1}K_{a2} = [\text{H}^+]^2[\mathbf{1}_{\text{-H}_2}]/[\mathbf{1}_{\text{-H}_4}{}^{2+}]$,

$$K_{\mathbf{1}\text{-}\mathbf{H}_2\text{-TMHQ}} = K_{\text{TMHQ-all}}/K_\beta \quad (5)$$

The free energy change for the protonation of $\mathbf{1}_{\text{-H}_2}$ by TMHQ ($\Delta G_{\text{1-H2-TMHQ}}$) is as follows:

$$\begin{aligned}\Delta G_{\mathbf{1}\text{-}\mathbf{H}_2\text{-TMHQ}} &= -RT\ln(K_{\text{TMHQ-all}}/K_\beta)\\ &= RT\ln 10 \times (\text{p}K_{\text{TMHQ-all}} - \text{p}K_\beta)\\ &= RT\ln 10 \times [\text{p}K_{\text{TMHQ-1}} + \text{p}K_{\text{TMHQ-2}} - (\text{p}K_{\text{a1}} + \text{p}K_{\text{a2}})]\end{aligned} \quad (6)$$

The experimentally obtained acid dissociation constant of $\mathbf{1}_{\text{-H}_4}{}^{2+}$ ($\text{p}K_\beta = \text{p}K_{\text{a1}} + \text{p}K_{\text{a2}} = 22.13$) is much smaller than the acid dissociation constant of phenol in THF (33.78).[33] Although the values of $\text{p}K_{\text{TMHQ-1}}$ and $\text{p}K_{\text{TMHQ-2}}$ in THF are not available, the minimum value can be set to 33.78 because TMHQ is assumed to be a weaker acid than phenol due to the electron-donating methyl groups in the phenyl ring. Furthermore, acid dissociation constant for production of a dianion from a monoanion is larger than that for production of the monoanion from a neutral species, resulting in $33.78 \le \text{p}K_{\text{TMHQ-1}} \le \text{p}K_{\text{TMHQ-2}}$. By using these values in eq 6, the value of $\Delta G_{\text{1-H2-TMHQ}}$ is calculated to be ≥259 kJ mol^{-1}. This value implies that path B is an extremely unfavorable process. The same discussion is applicable for the reaction with MMHQ because the acid dissociation constants for MMHQ are also larger than that of unsubstituted phenol.

Another possible way to trigger the reaction is the single-protonation to produce $\mathbf{1}_{\text{-H3}}{}^+$ followed by electron transfer (denoted as path B′, "sPT−ET mechanism"). However, it can be concluded that this process is also unlikely to occur according to the following discussion (the reaction with TMHQ is described as a representative example).

The equilibrium constant ($K_{\text{1-H2-TMHQ}}{}'$) for the single-protonation by TMHQ is as follows:

$$\begin{aligned}K_{\mathbf{1}\text{-}\mathbf{H}_2\text{-TMHQ}}{}' &= [\mathbf{1}_{\text{-H3}}{}^+][(\text{TMHQ-H})^-]/[\mathbf{1}_{\text{-H}_2}][\text{TMHQ}]\\ &= K_{\text{TMHQ-1}}/K_{\text{a1}} = 10^{(\text{p}K_{\text{a1}} - \text{p}K_{\text{TMHQ-1}})}\end{aligned} \quad (7)$$

The value of $\text{p}K_{\text{a1}}$ is not experimentally available, because the two protonation processes ($\mathbf{1}_{\text{-H}_2} \rightarrow \mathbf{1}_{\text{-H3}}{}^+$ and $\mathbf{1}_{\text{-H3}}{}^+ \rightarrow \mathbf{1}_{\text{-H}_4}{}^{2+}$) were not separately observed in the acid titration experiment ($n \sim 2$). Considering that production of a dianion is, in general, relatively uphill than that of a monoanion, $\text{p}K_{\text{a1}}$ should be larger than $\text{p}K_{\text{a2}}$, i.e., $\text{p}K_{\text{a1}} \ge \text{p}K_{\text{a2}}$. The difference between $\text{p}K_{\text{a1}}$ and $\text{p}K_{\text{a2}}$ is assumed to be $\text{p}K_{\text{a1}} - \text{p}K_{\text{a2}} \le 2$ because the similar titration procedures successfully demonstrated the separation of the two deprotonation processes of $\mathbf{2}_{\text{-H}_4}$ ($\Delta\text{p}K = 1.4$, see Figure 4). Under the following relationships

$$\text{p}K_{\text{a1}} + \text{p}K_{\text{a2}} = 22.13 \quad (8)$$

$$\text{p}K_{\text{a1}} \ge \text{p}K_{\text{a2}} \quad (9)$$

$$\text{p}K_{\text{a1}} - \text{p}K_{\text{a2}} \le 2 \quad (10)$$

dx.doi.org/10.1021/jo3013379 | J. Org. Chem. 2012, 77, 8946−8955

Scheme 7. Protonation of $\mathbf{1}_{\text{-H}_2}$ by TMHQ

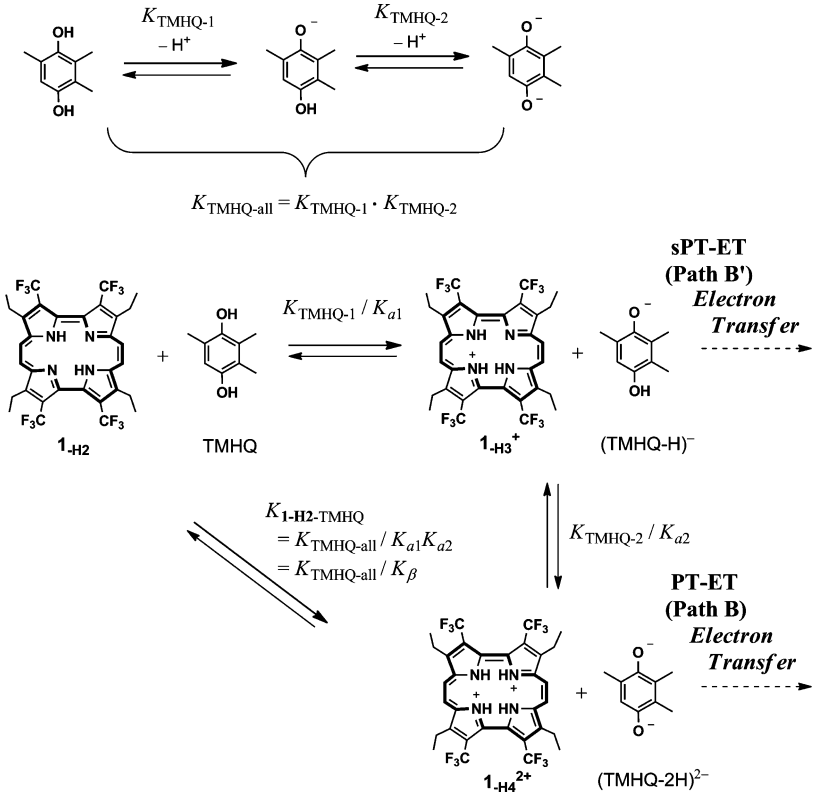

the value of pK_{a1} will be in the range of $pK_{a1} = 11-13$. In this case, the value of $K_{\text{1-H2-TMHQ}}'$ is calculated to be $K_{\text{1-H2-TMHQ}}' < 10^{-22.78}-10^{-20.78}$ (note that $pK_{\text{TMHQ-1}} \geq 33.78$). Taking the maximum value of $K_{\text{1-H2-TMHQ}}' = 10^{-20.78}$, this value of corresponds to +119 kJ mol^{-1}. Therefore, "sPT–ET" mechanism is unfavorable.

On the basis of the thermochemical analysis and the experimentally elucidated activation energy described above, the most likely reaction pathway is path C, i.e., concerted proton–electron transfer (CPET). The discussion described above is summarized in Figure 5, where the reaction with TMHQ is depicted as one example. The CPET mechanism requires preorganized arrangement of the reactants at the transition state, because protons and electrons should be transferred at the same time. This is reflected by the negative activation entropy with large absolute values. Furthermore, the observation of KIE also supports that the reaction proceeds via CPET.[22,23,36,37]

The KIE values for the reaction with MMHQ is smaller, compared with the value for the reaction with TMHQ. MMHQ is poorer in the reducing ability but more acidic, compared with TMHQ. The decrease in the KIE value might be originated from the partial switching in the reaction mechanism from a concerted pathway to a sequential pathway (i.e., pre-equilibrium proton transfer process followed by electron transfer) although the concerted mechanism is still dominant.

Evaluation of Free Energy Change between 18π/20π-Conjugation Mode. Thermochemical calculation based on acid dissociation constants and electrochemical data represent a popular approach for obtaining the bond dissociation enthalpy (BDE) or the bond dissociation free energy (BDFE) of an X–H bond (X = C, N, O, etc.).[38] The calculation procedure would also be applicable for evaluation of the free energy change in

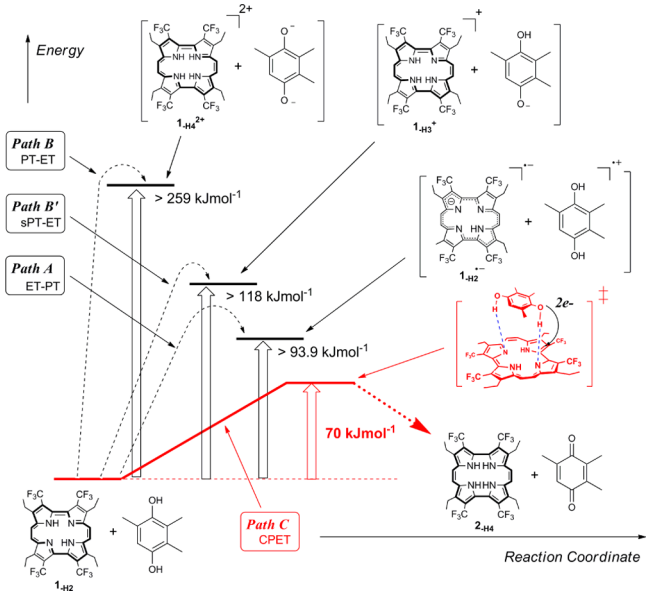

Figure 5. Choice of reaction pathway for the $\mathbf{1}_{\text{-H}_2}$ + TMHQ system.

the 18π/20π-conjugated CF_3 porphycene conversion. According to the procedures proposed by Bordwell[24,25] and Alice,[26,27] the free energy change, $\Delta G_{18\pi\rightarrow 20\pi}$, can be calculated in terms of hydrogen atom affinity:

$$\mathbf{1}_{\text{-H}_2} + 2\text{H}^{\bullet}(\equiv 2\text{H}^{+} + 2\text{e}^{-}) \rightarrow \mathbf{2}_{\text{-H}_4}(\text{free energy change:}\Delta G_{18\pi\rightarrow 20\pi}) \quad (11)$$

dx.doi.org/10.1021/jo3013379 | J. Org. Chem. 2012, 77, 8946–8955

Scheme 8. Elemental Processes of 18π/20π Conversion for Thermochemical Calculation

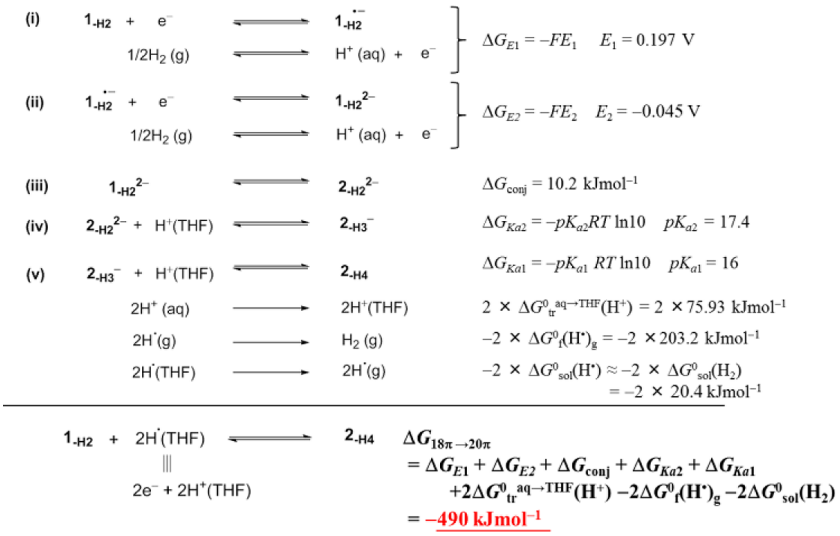

Elemental steps and free energy parameters for the 18π/20π-conversion are summarized in Scheme 8.

The redox potentials (E_1 and E_2) were employed as the values vs SHE. ΔG_{conj} is the free energy change between dianion forms ($\mathbf{1}_{\text{-}H_2}^{2-}$ and $\mathbf{2}_{\text{-}H_2}^{2-}$), which is evaluated by the DFT calculation. The value of $\Delta G^0_{tr}{}^{aq\rightarrow THF}(H^+)$ is the free energy required to transfer a proton from water to THF (= +75.93 kJ mol^{-1}).[39] The value of $\Delta G^0_f(H^\bullet)_g$, the free energy of formation of hydrogen atom in gas phase, was taken as the reported value of 203.2 kJ mol^{-1} (= 48.58 kcal mol^{-1}).[40] The solvation energy of a hydrogen atom, $\Delta G^0_{sol}(H^\bullet)$, was assumed to be the same as that of a hydrogen molecule ($\Delta G^0_{sol}(H_2)$) and calculated from the mole fraction solubility of hydrogen gas in THF at 1 atm:[25]

$$\Delta G^0_{sol}(H^\bullet) \approx \Delta G^0_{sol}(H_2) = -RT\ \ln(\chi_{H2}) \qquad (12)$$

where χ_{H2} is the mole fraction solubility of hydrogen gas in THF at 298.15 K under 1 atm (= 2.7×10^{-4})[41] and $\Delta G^0_{sol}(H^\bullet)$ is calculated to be 20.4 kJ mol^{-1}.

The thermochemical calculation yields $\Delta G_{18\pi\rightarrow20\pi}$ = −490 kJ mol^{-1},[42] indicating that the formation of the 20π-conjugated CF_3 porphycene is thermodynamically favorable in spite of the loss of aromaticity. Considering that $-\Delta G_{18\pi\rightarrow20\pi}$ (= +490 kJ mol^{-1}) corresponds to the BDFE for *two* N−H bonds in $\mathbf{2}_{\text{-}H_4}$, it will be recognized that the N−H bonds are rather accessible to cleavage: BDFEs of *one* N−H bond in 2- and/or 5-substituted pyrroles are in the range from 380−450 kJ mol^{-1}.[43] The value of $-\Delta G_{18\pi\rightarrow20\pi}$ determined in this research indicates that *one* N−H bond in $\mathbf{2}_{\text{-}H_4}$ can be cleaved by almost half of the energy required for cleavage of an N−H bond in a pyrrole. One of the reasons for the small BDFE is the attainment of π-electron delocalization in $\mathbf{2}_{\text{-}H_4}$, i.e., antiaromaticity. The π-electron delocalization throughout whole of macrocycle will stabilize (a) radical(s) or (a) negative charge(s) formed by N−H bond cleavage, compared with single pyrrole unit.

Antiaromatic molecules generally tend to take more stable nonaromatic forms through structural deformation.[21] In a completely deformed and nonaromatic structure, the higher energy to cleave the N−H bonds (large BDFE) must be required, because the effective stabilization of (a) radical(s) or (a) negative charge(s) formed at the transition state cannot be expected. Antiaromaticity of $\mathbf{2}_{\text{-}H_4}$ with 20π-conjugated delocalization character contributes to both the destabilization of the ground state and the stabilization of the transition state during the N−H bond cleavage.

Driving Force for the Reaction of $\mathbf{1}_{\text{-}H_2}$ with Hydroquinones: Thermochemical Analysis for the Entire Reaction. In a reaction accompanying dissociations of hydrogen atoms, the BDFE data of chemical species are useful for evaluating the driving force of the reaction. When the procedure is applied for the reaction of $\mathbf{1}_{\text{-}H_2}$ with TMHQ in THF (depicted in Scheme 1), the free energy change is evaluated by the difference between the BDFEs of $\mathbf{2}_{\text{-}H_4}$ and TMHQ ($BDFE_{TMHQ} - BDFE_{1\text{-}H2}$), where both the parameters include the total energies for the dissociation of two hydrogen atoms (see Scheme 9). The biradical form produced from TMHQ is chemically equivalent to trimethyl *p*-benzoquinone (TMBQ).

Scheme 9. Bond Dissociations in $\mathbf{1}_{\text{-}H_2}$ and TMHQ

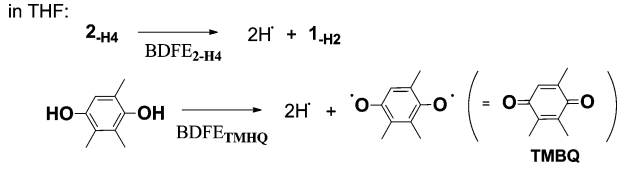

As described above, $BDFE_{2\text{-}H4}$ can be set to 490 kJ mol^{-1}. $BDFE_{TMHQ}$ value in THF may be estimated from the electrochemical data shown in Figure S5, Supporting Information. Assuming that the observed anodic wave in the cyclic voltammogram of TMHQ is attributed to the 2e$^-$-oxidation coupled with 2H$^+$ release,[44] the $BDFE_{TMHQ}$ value (for two O−H bonds) was estimated to be 521 kJ mol^{-1} according to the procedure described in the Supporting Information. This value implies that the average energy for the cleavage of *one* O−H bond of TMHQ is 260.5 kJ mol^{-1} (= 62.2 kcalmol^{-1}). BDFE values in lower polar solvents are, in general, expected to be smaller than those in water.[23] Because the obtained value is smaller than the average energy for the cleavage of *one* O−H bond of TMHQ in water (292 kJ mol^{-1} (= 69.8 kcalmol^{-1})),[23]

dx.doi.org/10.1021/jo3013379 | J. Org. Chem. 2012, 77, 8946−8955

the calculated value would be in the reasonable range of energies. Even if uncertainty of the calculated BDFE value derived from and the errors in the free energies for phase transfer of a proton and hydrogen gas (~5% at maximum) is considered, it may be concluded from the BDFE-based analysis that the reaction of $\mathbf{1}_{\text{-H}_2}$ with TMHQ is thermodynamically uphill by 31 kJ mol^{-1}. However, the reaction, in fact, proceeds as demonstrated above. The inconsistency between the experimental fact and the thermochemical analysis suggests that some factors which are not reflected in the BDFE-based analysis should be taken into consideration.

One possible factor is multipoint specific interactions between chemical species at the initial state and/or at the final state (product state). BDFEs-based analysis, in general, focuses on the difference in the BDFEs of chemical species participating in the reaction, where each BDFE value is independently determined. This kind of analyses assumes a simple collision or a single-point contact between the reactants during reaction. In contrast, the reaction of $\mathbf{1}_{\text{-H}_2}$ with TMHQ proceeds with the multipoint contacts through the two [($\mathbf{1}_{\text{-H}_2}$: pyrrole)N---H−O(TMHQ)] moieties. The significance of the multipoint contacts is supported by the choice of reaction pathway: Any stepwise mechanism is found to be unfavorable. Structural perturbation in the framework of $\mathbf{1}_{\text{-H}_2}$ will be induced by the access of TMHQ to $\mathbf{1}_{\text{-H}_2}$ through the multipoint contacts, which would destabilize $\mathbf{1}_{\text{-H}_2}$ especially in the presence of huge excess of TMHQ. At the product state, the two hydrogen bonds at the [($\mathbf{2}_{\text{-H}_4}$: pyrrole)N−H---O═C(TMBQ)] moieties are transiently formed, which is converted into [($\mathbf{2}_{\text{-H}_4}$: pyrrole)N−H---O(THF)] hydrogen bonds.[45] The [($\mathbf{2}_{\text{-H}_4}$: pyrrole)N−H---O═C(TMBQ)] hydrogen bond at the product state would be stronger than [($\mathbf{1}_{\text{-H}_2}$: pyrrole)N---H−O(TMHQ)] at the initial state because the pyrrolic nitrogen atoms in $\mathbf{1}_{\text{-H}_2}$ are associated with the aromatic π-conjugation and the hydrogen bonds with the inner protons.[46] The multipoint hydrogen bonds at the product state will contribute to the stabilization of the energy level of the product state, which cannot be reflected in a simple BDFE-based analysis. Although more studies are required to test the BDFE-based approach for evaluating the driving force of a reaction accompanying multipoint contacts of reactants by investigating various cases, it may be concluded that the contact modes of chemical species at the initial and/or the product states can significantly affect the entire energy profile in a reaction.

CONCLUSION

The reaction of the 18π-conjugated trifluoromethylated porphycene with a hydroquinone reagent to produce the corresponding 20π-conjugated form proceeds via CPET. This pathway is taken as a result of the high energy barriers in the one-electron transfer reaction from a hydroquinone to the 18π-conjugated porphycene and in the thermodynamically unfavorable protonation of the inner nitrogen atoms. According to the thermochemical calculations for the conversion of the 18π-conjugated trifluoromethylated porphycene into the 20π-conjugated form, the process is thermodynamically favorable. We demonstrated that investigation with a combination of kinetic and thermochemical analyses is applicable for addressing the reaction pathway for the conversion of aromaticity/non- or antiaromaticity in porphyrinoids. The knowledge obtained here will give us procedures for predicting the experimental availability of unknown π-conjugated compounds and clear insights into molecular design strategies for preparing and isolating porphyrinoids with unique π-conjugation modes.

EXPERIMENTL SECTION

Instruments. ^{1}H NMR spectra were obtained by using a 400 MHz spectrophotometer. The peak assignments were conducted with reference to the previous report[20] and doubly checked by D_2O exchange and COSY method. UV−vis experiments and kinetic measurements were conducted on a double beam spectrophotometer equipped with a thermostat cell holder within a deviation of 0.1 °C. Cyclic voltammetry measurements were carried out using a cyclic voltammeter with a glassy carbon electrode as the working electrode, a platinum wire as the counter electrode and a Ag/AgPF$_6$ electrode as the reference electrode.

Materials. THF was dried on sodium and obtained through vacuum transfer. Other chemicals were used as received. 2,7,12,16-Tetraethyl-3,6,13,16-tetrakis(trifluoromethyl)porphycene $\mathbf{1}_{\text{-H}_2}$[28,29] was synthesized by previous described methods. The 20π-conjugated form, $\mathbf{2}_{\text{-H}_4}$, was obtained from $\mathbf{1}_{\text{-H}_2}$ by the reaction with excess amount of a hydroquinone reagent in THF and purified by alumina chromatography with elution of CH_2Cl_2 in the same manner as the reported method:[20] ^{1}H NMR (400 MHz, THF-d_8, TMS) δ = 11.36 (1H, br, exchangeable with D_2O), 6.03 (s, 4H), 2.57 (8H, q, J = 7.6 Hz), 1.14 (12H, t, J = 7.6 Hz); ^{13}C NMR (100 MHz, $CDCl_3$, TMS) δ = 128.12, 127.02, 123.35(q, $^1J_{CF}$ = 268.7 Hz), 119.34, 115.17(q, $^2J_{CF}$ = 36.2 Hz), 112.94, 68.14, 26.13, 17.69, 15.99; ^{19}F NMR (376 MHz, THF-d_8, C_6F_6 (−164.6 ppm)) δ = −54.52; HRMS-FAB calcd for [M$^+$] $C_{32}H_{30}N_4F_{12}^+$ 696.2122, found 696.2128; UV−vis λ_{max} nm (ε, M^{-1} cm^{-1}) in THF 291 (3.8×10^4), 323 (4.1×10^4), 381 (sh, 3.3×10^3), 609 (2.9×10^2), 691 (3.0×10^2), 708 (3.2×10^2).

Determination of Reaction Stoichiometry. The stoichiometry of the reaction of $\mathbf{1}_{\text{-H}_2}$ with 2,3,5-trimethylhydroquinone (TMHQ) was determined using UV−vis and ^{1}H NMR spectroscopies. In the UV−vis measurements, a solution of $\mathbf{1}_{\text{-H}_2}$ (15 μM) in dry THF was incubated at 25 °C under a N_2 atmosphere. The decreases in the absorbance at 375 nm measured at 22 h after addition of TMHQ (0 − 50 μM) into the solution of $\mathbf{1}_{\text{-H}_2}$ were plotted against [TMHQ]/[$\mathbf{1}_{\text{-H}_2}$]. In the ^{1}H NMR measurements, a solution of $\mathbf{1}_{\text{-H}_2}$ in dry THF was mixed with TMHQ (final concentrations: [$\mathbf{1}_{\text{-H}_2}$] = 1.3 mM, [TMHQ] = 0.46, 1.1, or 1.4 mM) at 25 °C under a N_2 atmosphere. After 12 h, the solvent was evaporated and dioxane and CD_3CN (5%(v/v)) were added. The solutions were subjected to ^{1}H NMR measurements using peak presaturation method to diminish the peak intensities originated from dioxane protons. Dioxane was necessary to increase the solubility of the products ($\mathbf{2}_{\text{-H}_4}$ and trimethyl p-benzoquinone).

Kinetic Measurement for Reaction of $\mathbf{1}_{\text{-H}_2}$ with Substituted Hydroquinones. For kinetic measurements, two kinds of hydoquinones were employed (TMHQ and monomethyl hydroquinone (MMHQ)). In a 1-cm path quartz cell equipped with a three-way stopcock, a solution of $\mathbf{1}_{\text{-H}_2}$ in dry THF was incubated at 25 °C under a N_2 atmosphere. After addition of excess TMHQ or MMHQ dissolved in THF, the absorbance change at 720 nm was monitored. The reaction curves were analyzed by single-phase kinetic law to obtain the pseudo-first-order rate constants. The concentrations of the reactants in final were [$\mathbf{1}_{\text{-H}_2}$] = 3.5 μM and [TMHQ] or [MMHQ] = 0−0.3 mM ([hydroquinone] > 10 × [$\mathbf{1}_{\text{-H}_2}$] was kept). The activation parameters were obtained by an Eyring plot in the range from −10 to +40 °C.

The kinetic isotope effect (KIE) was determined by k_H/k_D, where k_H and k_D are the rate constants obtained in 95% THF + 5% CH_3OH and in 95% THF + 5% CD_3OD, respectively. The deuteration ratio of the phenolic protons of TMHQ and MMHQ in the presence of 5%

dx.doi.org/10.1021/jo3013379 | J. Org. Chem. 2012, 77, 8946−8955

CD_3OD are 74% and 91% (evaluated by ^1H NMR spectroscopy), respectively. Accordingly, the observed reaction profiles obtained in 95% THF + 5% CD_3OD were analyzed by the formula $k_{d,obs} = k_H(1 - f_D) + k_D f_D$, where $k_{d,obs}$ is the observed rate constant and f_D is the fraction of deuterium in a hydroquinone (= 0.74 for TMHQ and 0.91 for MMHQ).[47] The concentrations of the reactants were $[\mathbf{1}_{\text{-}H_2}] = 3.5$ μM, [TMHQ] = 1.8 mM, and [MMHQ] = 11.2 mM.

Electrochemical Measurement. The cyclic voltammogram was obtained in the range from −1.2 to 0 V (for $\mathbf{1}_{\text{-}H_2}$) or 0 V to +1.0 V (for TMHQ and MMHQ) (vs Ag/0.01 M $AgPF_6$) with a scan speed of 0.1 V/s in the presence of 0.1 M Bu_4NPF_6. The potentials were calibrated by using the redox couple of ferrocene/ferronenium cation ($E_{p/2}$ = +0.56 V vs SCE)[48] and converted into values vs SHE by adding 0.241 V.

Acid Titration toward $\mathbf{1}_{\text{-}H_2}$. A solution of $\mathbf{1}_{\text{-}H_2}$ (4 μM) was titrated with methanesulfonic acid (MSA) in THF and the spectral changes were followed by UV−vis spectroscopy. The procedure used to determine the acid dissociation constants was performed according to a method described in a previous report on the protonation of corroles.[49] The absorbance change at 372 nm was analyzed using a modified Hill plot for determination of the acid dissociation constant in the same manner as the investigation of a porphyrin−ligand complexation[50,51]

$$\begin{aligned}&\log[(Z - A_{\text{neutral}})/(A_{\text{acidic}} - Z)]\\ &= n\log[\text{MSA}] + (\log K_{a(\text{MSA})} - \log K_{ai})\\ &= n\log[\text{MSA}] + (\text{p}K_{ai} - \text{p}K_{a(\text{MSA})}),\ i = 1, 2\end{aligned} \tag{13}$$

where Z is the absorbance at each concentration of the acid, A_{neutral} is the absorbance of the $\mathbf{1}_{\text{-}H_2}$ form, A_{acidic} is the absorbance of a protonated form ($\mathbf{1}_{\text{-}H3}^{+}$ or $\mathbf{1}_{\text{-}H_4}^{2+}$), n is the number of transferred protons, $K_{a(\text{MSA})}$ is the acid dissociation constant of MSA ($\text{p}K_{a(\text{MSA})}$ = 13.53 in THF[33]), and K_{ai} is the acid dissociation constant of $\mathbf{1}_{\text{-}H3}^{+}$ (i = 1) or $\mathbf{1}_{\text{-}H_4}^{2+}$ (i = 2). However, since it was found in this research that $\text{p}K_{a1}$ and $\text{p}K_{a2}$ cannot be separately determined ($n \sim 2$), the overall acid dissociation constant ($K_\beta = K_{a1}K_{a2}$) was obtained using the following equation:

$$\begin{aligned}&\log[(Z - A_{\text{neutral}})/(A_{\text{acidic}} - Z)]\\ &= 2\log[\text{MSA}] + [\log K_{a(\text{MSA})} - \log(K_{a1}K_{a2})]\\ &= 2\log[\text{MSA}] + (p K_\beta - \text{p}K_{a(\text{MSA})})\end{aligned} \tag{14}$$

Base Titration toward $\mathbf{2}_{\text{-}H_4}$. A solution of $\mathbf{2}_{\text{-}H_4}$ (4 μM) was titrated with 1,8-diazabicyclo[5.4.0]undec-7-ene (DBU). The absorbance change at 324 nm was plotted against log[DBU] to obtain the value of $\text{p}K'_{a1}$ and $\text{p}K'_{a2}$, where K'_{a1} is the acid dissociation constant of $\mathbf{2}_{\text{-}H_4}$, and K'_{a2} is the acid dissociation constant of $\mathbf{2}_{\text{-}H3}$. The plot of absorbance at 324 nm against log[DBU] is composed of two phases. The first stage (low [DBU] regions) was analyzed to obtain the value of $\text{p}K'_{a1}$ according to the following equation

$$\begin{aligned}&\log[(Z' - A'_{H4})/(A'_{H3} - Z')]\\ &= \log[\text{DBU}] + (\log K'_{a1} - \log K_{a(\text{DBU})})\\ &= \log[\text{DBU}] + (\text{p}K_{a(\text{DBU})} - \text{p}K'_{a1})\end{aligned} \tag{15}$$

where Z' is the absorbance at each concentration of DBU, A'_{H4} is the absorbance of the $\mathbf{2}_{\text{-}H_4}$ form, A'_{H3} is the absorbance of the deprotonated form, $\mathbf{2}_{\text{-}H3}^{-}$, $K_{a(\text{DBU})}$ is the acid dissociation constant of the conjugated acid of DBU ($\text{p}K_{a(\text{DBU})}$ = 19.97 in THF[52]), and K'_{a1} is the acid dissociation constant of $\mathbf{2}_{\text{-}H_4}$. The value of A'_{H3} was set as the best fit value to yield the maximum correlation coefficient in the analysis of eq 15. The high [DBU] region was analyzed to elucidate the value of $\text{p}K'_{a2}$ according to eq 16

$$\begin{aligned}&\log[(Z' - A'_{H3})/(A'_{H2} - Z')]\\ &= \log[\text{DBU}] + (\log K'_{a2} - \log K_{a(\text{DBU})})\\ &= \log[\text{DBU}] + (\text{p}K_{a(\text{DBU})} - \text{p}K'_{a2})\end{aligned} \tag{16}$$

where A'_{H2} is the absorbance upon completion of the titration (determined by the addition of a large excess of DBU).

Evaluation of Free Energy Difference between Dianion Forms ($\mathbf{1}_{\text{-}H_2}^{2-}$ and $\mathbf{2}_{\text{-}H_2}^{2-}$). The difference in the free energy between $\mathbf{1}_{\text{-}H_2}^{2-}$ and $\mathbf{2}_{\text{-}H_2}^{2-}$ was evaluated by DFT calculation by Spartan '08 (Wave function, Inc.). The B3LYP function with the LANL2DZ and 6-31G* basis set was employed for the calculations.[53] The energy values are described as total energies including heat formation energies and steric energies. The calculations were started from the structure of $\mathbf{2}_{\text{-}H_4}$ obtained by X-ray crystallography.

■ ASSOCIATED CONTENT

Ⓢ Supporting Information

Calculation of $BDFE_{TMHQ}$, determination of reaction stoichiometry by ^1H NMR measurement, spectral changes during the reaction of $\mathbf{1}_{\text{-}H_2}$ with MMHQ, Eyring plot, evaluation of kinetic isotope effect, cyclic voltammograms, and computed structures of dianion forms. This material is available free of charge via the Internet at http://pubs.acs.org.

■ AUTHOR INFORMATION

Corresponding Author

*E-mail: tmatsuo@ms.naist.jp, thayashi@chem.eng.osaka-u.ac.jp.

Notes

The authors declare no competing financial interest.

■ ACKNOWLEDGMENTS

This work was supported by a Grant-in-Aid for Science Research for Young Scientists (B) (T.M.) and a Grant-in-Aid for Science Research on Innovative Areas (Molecular Activation Directed toward Straightforward Synthesis) from MEXT Japan (T.M. and T.H.). T.M. acknowledges Prof. Shun Hirota and Mr. Leigh McDowell (Nara Institute of Science and Technology) for his encouragement to prepare this paper.

■ REFERENCES

(1) Stępień, M.; Latos-Grażyński, L. In *Topics in Hetercyclic Chemsitry 19. Aromaticity in Heterocyclic Compounds*; Gupta, R. R., Ed.; Springer-Verlag Berlin Heidelberg: Heidelberg, Germany, 2009, p 83−153.
(2) Sessler, J. L.; Gebauer, A.; Vogel, E. In *The Porphyrin Handbook*; Kadish, K. M., Smith, K. M., Guilard, E., Eds.; Academic Press: San Diego, 2000; Vol. *1*, p 1.
(3) Wiberg, K. B. *Chem. Rev.* **2001**, *101*, 1317−1331.
(4) Paolesse, R. In *Porphyrin Handbook*; Kadish, K. M., Smith, K. M., Guilard, R., Eds.; Academic Press: San Diego, 2000; Vol. *2*, pp 201−232.
(5) Yoon, Z. S.; Kwon, J. H.; Yoon, M. C.; Koh, M. K.; Noh, S. B.; Sessler, J. L.; Lee, J. T.; Seidel, D.; Aguilar, A.; Shimizu, S.; Suzuki, M.; Osuka, A.; Kim, D. *J. Am. Chem. Soc.* **2006**, *128*, 14128−14134.
(6) Vogel, E.; Kocher, M.; Schmickler, H.; Lex, J. *Angew. Chem., Int. Ed.* **1986**, *25*, 257−259.
(7) Callot, H. J.; Rohrer, A.; Tschamber, T.; Metz, B. *New. J. Chem.* **1995**, *19*, 155−159.
(8) Setsune, J.-i.; Katakami, Y.; Iizuna, N. *J. Am. Chem. Soc.* **1999**, *121*, 8957−8958.
(9) Stępień, M.; Latos-Grażyński, L.; Szterenberg, L. *J. Org. Chem.* **2007**, *72*, 2259−2270.

(10) Yamamoto, Y.; Hirata, Y.; Kodama, M.; Yamaguchi, T.; Matsukawa, S.; Akiba, K. Y.; Hashizume, D.; Iwasaki, F.; Muranaka, A.; Uchiyama, M.; Chen, P.; Kadish, K. M.; Kobayashi, N. *J. Am. Chem. Soc.* **2010**, *132*, 12627−12638.
(11) Shimizu, S.; Shin, J. Y.; Furuta, H.; Ismael, R.; Osuka, A. *Angew. Chem., Int. Ed.* **2003**, *42*, 78−82.
(12) Sessler, J. L.; Seidel, D.; Vivian, A. E.; Lynch, V.; Scott, B. L.; Keogh, D. W. *Angew. Chem., Int. Ed.* **2001**, *40*, 591−594.
(13) Liu, C.; Shen, D.-M.; Chen, Q.-Y. *J. Am. Chem. Soc.* **2007**, *129*, 5814−5815.
(14) Brothers, P. J. *Chem. Commun.* **2008**, 2090−2102.
(15) Cissell, J. A.; Vaid, T. P.; Yap, G. P. A. *Org. Lett.* **2006**, *8*, 2401−2404.
(16) Stepien, M.; Latos-Grazynski, L.; Sprutta, N.; Chwalisz, P.; Szterenberg, L. *Angew. Chem., Int. Ed.* **2007**, *46*, 7869−7873.
(17) Shin, J. Y.; Kim, K. S.; Yoon, M. C.; Lim, J. M.; Yoon, Z. S.; Osuka, A.; Kim, D. *Chem. Soc. Rev.* **2010**, *39*, 2751−2767.
(18) Woodward, R. B. *Angew. Chem.* **1960**, *72*, 651−652.
(19) Kuzuhara, D.; Yamada, H.; Yano, K.; Okujima, T.; Mori, S.; Uno, H. *Chem.—Eur. J.* **2011**, *17*, 3376−3383.
(20) Matsuo, T.; Ito, K.; Kanehisa, N.; Hayashi, T. *Org. Lett.* **2007**, *9*, 5303−5306.
(21) Kim, K. S.; Sung, Y.-H.; Matsuo, T.; Hayashi, T.; Kim, D. *Chem.—Eur. J.* **2011**, *17*, 7882−7889.
(22) Mayer, J. M. *Acc. Chem. Res.* **2010**, *44*, 36−46.
(23) Warren, J. J.; Tronic, T. A.; Mayer, J. M. *Chem. Rev.* **2010**, *110*, 6961−7001.
(24) Bordwell, F. G. *Acc. Chem. Res.* **1988**, *21*, 456−463.
(25) Bordwell, F. G.; Cheng, J. P.; Harrelson, J. A. *J. Am. Chem. Soc.* **1988**, *110*, 1229−1231.
(26) Parker, V. D. *J. Am. Chem. Soc.* **1992**, *114*, 7458−7462.
(27) Wayner, D. D. M.; Parker, V. D. *Acc. Chem. Res.* **1993**, *26*, 287−294.
(28) Hayashi, T.; Nakashima, Y.; Ito, K.; Ikegami, T.; Aritome, I.; Aoyagi, K.; Ando, T.; Hisaeda, Y. *Inorg. Chem.* **2003**, *42*, 7345−7347.
(29) Hayashi, T.; Nakashima, Y.; Ito, K.; Ikegami, T.; Aritome, I.; Suzuki, A.; Hisaeda, Y. *Org. Lett.* **2003**, *5*, 2845−2848.
(30) In electrochemical measurement of hydroquinone in aprotic solvent, the first anodic (oxidation) wave is assgned as a two-electron oxidation coupled with deprotonation to form the benzoquinone form. Eggins, B. R.; Chamers, J. Q. *J. Electrochem. Soc.* **1970**, *117*, 186−192.
(31) Binstead, R. A.; McGuire, M. E.; Dovletoglou, A.; Seok, W. K.; Roecker, L. E.; Meyer, T. J. *J. Am. Chem. Soc.* **1992**, *114*, 173−186.
(32) Laviron, E. *J. Electroanal. Chem.* **1984**, *164*, 213−227.
(33) Ding, F.; Smith, J. M.; Wang, H. *J. Org. Chem.* **2009**, *74*, 2679−2691.
(34) Schleyer, P. V.; Maerker, C.; Dransfeld, A.; Jiao, H. J.; Hommes, N. J. R. V. *J. Am. Chem. Soc.* **1996**, *118*, 6317−6318.
(35) Other terms for this reaction mode have been used (e.g., proton-coupled electron transfer, electron-coupled proton transfer, etc.). In this work, the term "concerted proton−electron transfer" is employed because the discussion issue is focused on whether protons and electrons move stepwise or at the same time.
(36) Hammes-Schiffer, S.; Stuchebrukhov, A. A. *Chem. Rev.* **2010**, *110*, 6939−6960.
(37) Markle, T. F.; Rhile, I. J.; Mayer, J. M. *J. Am. Chem. Soc.* **2011**, *133*, 17341−1735.
(38) BDE values are often reported as enthalpic energies in gas phase, whereas BDFE values include entropic contributions. The values evaluated from the electrochemical/acid dissociation data here are expressed as "BDFE" because the difference in the entropic term between the 18/20π-conjugated compounds is not negligible because of the large change in the conformations.
(39) Elsemongy, M. M.; Abdel-Khalek, A. A. *Thermophys. Acta* **1991**, *181*, 79−94.
(40) Nicholas, A. M. D.; Arnold, D. R. *Can. J. Chem.* **1982**, *60*, 2165−2179.
(41) Brunner, E. *J. Chem. Eng. Data* **1985**, *30*, 269−273.
(42) Tilset reported the value of $-\Delta G^0_{tr}{}^{aq\rightarrow THF}(H^+) + \Delta G^0_f(H^\bullet) + \Delta G^0_{sol}(H^\bullet)$ as 276 kJ mol^{-1} for calculation of BDEs, based on redox pontentials with the reference of ferrocene/ferrocenium electrode and thermochemical paramaters in pseudoaqueous solutions. Tilset, M. In *Comprehensive Organometallic Chemistry III*; Crabtree, R. H., Mingos, M. D. P., Eds.; Elsevier: Amsterdam, 2006; Vol. *1*, pp 279−305.
(43) Luo, Y.-R. In *Comprehensive Handbook of Chemical Bond Energies*; CRC Press: Boca Raton, 2007; pp 369−424.
(44) As descibed in ref 30, the previous report on electrochemistry of hydroquinones in organic solvent has assigned the first anodic wave as the oxidation of a hydroquinone form to a benzoquinone form. Stricly speaking, confirmation of the assignment by electrochemical measurement in the presence of acids would be required in this work. However, for estimating the *average* value of BDFE, the assumtion does not affect the following discussion because the second oxidation for hydroquinones, in general, occurs at more negative potential and the acidity of the semiquinone form formed by the first oxidation is more acidic than TMHQ.
(45) It is experimentlly impossible to detect the TMBQ adduct of $\mathbf{2}_{\mathbf{H_4}}$ in concetrations under typical measurement conditions. This is because a large excess of THF molecules readily replace TMBQ.
(46) Waluk, J. *Acc. Chem. Res.* **2006**, *39*, 945−952.
(47) Rhile, I. J.; Mayer, J. M. *J. Am. Chem. Soc.* **2004**, *126*, 12718−12719.
(48) Geiger, W. E.; Ohrenberg, N. C.; Yeomans, B.; Connelly, N. G.; Emslie, D. J. *J. Am. Chem. Soc.* **2003**, *125*, 8680−8688.
(49) Ou, Z.; Shen, J.; Shao, J.; E, W.; Gałęzowski, M.; Gryko, D. T.; Kadish, K. M. *Inorg. Chem.* **2007**, *46*, 2775−2786.
(50) Brault, D.; Rougee, M. *Biochemistry* **1974**, *13*, 4591−4597.
(51) McLees, B. D.; Caughey, W. S. *Biochemistry* **1968**, *7*, 642−652.
(52) Garrido, G.; Koort, E.; Ràfols, C.; Bosch, E.; Rodima, T.; Leito, I.; Rosés, M. *J. Org. Chem.* **2006**, *71*, 9062−9067.
(53) Lee, C.; Yang, W.; Parr, R. G. *Phys. Rev. B* **1988**, *37*, 785−789.